

Effect of Heat and Mass Transfer on Casson Fluid Flow Between Two Co-Axial Tubes with Peristalsis

Open
Access

Nabil Tawfik Eldabe^{1,*}, Mohamed Yahya Abouzeid¹, Hemat A. Ali²

¹ Department of Mathematics, Faculty of Education, Ain Shams University, Roxy, Heliopolis, Cairo, Egypt

² Department Mathematics, Faculty of Science, Zagazig University, Zagazig, Egypt

ARTICLE INFO

ABSTRACT

Article history:

Received 22 June 2020

Received in revised form 17 July 2020

Accepted 23 July 2020

Available online 8 October 2020

The effects of both Hall currents and radiation on unsteady flow of an incompressible non-Newtonian fluid obeying Casson model through a porous medium have been discussed. The thermal-diffusion and diffusion thermo effects are taken into our consideration. The non-linear partial differential equations which govern this problem are simplified by assuming of long wavelength and small Reynolds number. These equations are solved numerically by using explicit finite difference method. In addition, the axial velocity, temperature and concentration are illustrated graphically for various parameters of the problem such as magnetic parameter (Hartman number), the upper limit apparent viscosity coefficient, Hall parameter, the pressure gradient, Prandtl number, Eckert number, Darcy number, Dufour number, the radiation parameter, Schmidt number, Soret number, the chemical reaction parameter and heat source/sink parameter. Furthermore, it is noticed that the behavior of the pressure gradient and Hartman number parameters is to increase or decrease the temperature distributions and is quite revers.

Keywords:

Hall currents; Peristaltic flow; Heat and mass transfer; Non-Newtonian fluid; Porous medium

Copyright © 2020 PENERBIT AKADEMIA BARU - All rights reserved

1. Introduction

In fluid mechanics, the boundary layer is considered as an essential part and indicates to the layer of fluid in the immediate vicinity of a bounding surface where the effects of viscosity are considerable. A range of velocities occurs across the boundary layer from maximum to zero, provided that the fluid is in contact with the surface. The expansion of boundary layer velocity on a flat plate was first scrutinized by Blasius [1] and that's expansion of velocity have been studied through this paper. In recent years. Considerable attention has been devoted to the study of boundary layer flow behavior and heat transfer characteristics of a non-Newtonian fluid past a vertical plate because of its extensive applications in engineering processes. Howarth [2] discussed the various aspects of the

* Corresponding author.

E-mail address: eldabe_math@yahoo.com

<https://doi.org/arfmts.76.1.5475>

Blasius flat plate flow problem numerically while, our paper use two different semi-analytical methods. The boundary layer equations play a central role in many aspects of fluid mechanics since they design the motion of a viscous fluid near the surface. The heat transfer for problem that offered by Howarth [2] was computed by Pohlhausen [3]. Abouzeid [4] studied the heat generation and viscous dissipation effects on a Newtonian fluid over a stretching sheet with heat transfer. Eldabe *et al.*, [5] discussed effects of uniform magnetic field, heat generation and chemical reaction on the flow of non-Newtonian nanofluid down a vertical cylinder. For more theorems and investigation see Refs. [6-10].

The transportation of fluid by a wave of contraction and expansion from a region of lower pressure to higher pressure is called peristaltic pumping. The study of peristaltic motion gained considerable interest because of its extensive applications. It is an inherent property of many biological systems. In living system, it is a distinctive pattern of smooth muscle contractions that propel the contents of the tube, as foodstuffs through esophagus and alimentary canal, urine from kidneys to bladder and other glandular ducts. The mechanism of peristaltic transport has been exploited for industrial applications like sanitary fluid transport, blood pumps in heart lung machine and transport of corrosive fluids where the contact of the fluid with the machinery parts is prohibited. This mechanism is used also in engineering devices like finger pumps and roller pumps. The investigation of the effects of wall properties on peristaltic transport of a dusty fluid was done by Srinivasacharya *et al.*, [1]. Peristaltic MHD flow of a Bingham fluid through a porous medium in a channel has been studied by Suryanarayana *et al.*, [2]. Peristaltic motion with heat transfer of a power-law nanofluid through a nonuniform inclined tube was analyzed by Abouzeid and Mohamed [3]. Mekheimer *et al.*, [4] investigated the influence of heat transfer and magnetic field on peristaltic transport of Newtonian fluid in a vertical annulus: application of an endoscope.

Theory of non-Newtonian fluid has received a great attention during the recent years because the traditional viscous fluids cannot precisely describe the characteristics of many physiological fluids. Eldabe *et al.*, [5] have studied the problem of MHD a thin-film transport of non-Newtonian fluid with heat and mass transfer down a vertical cylinder. The problem of wall properties and coupled stress effects on heat and mass transfer of peristaltic fluid flow through a porous medium is the problem of Wall properties and coupled stress effects on heat and mass transfer of peristaltic fluid flow through a porous medium by El-dabe *et al.*, [6]. The peristaltic pumping of a non-Newtonian fluid was analyzed by Medhavi [7]. Peristaltic transport of Casson fluid in a channel is discussed by Nagarani and Sarojamma [8]. Mansour and Abouzeid [9] illustrated the effects of heat and mass transfer on MHD flow of an incompressible biviscosity fluid in a non-uniform vertical tube.

The Hall effect is important when the Hall parameter which is ratio between the electron-cyclotron frequency and the electron-atom-collision frequency is high, this can occur if the collision frequency is low or when the magnetic field is high. This is a current trend in magnetohydrodynamics because of its important influence on the electromagnetic force. Hence, it is important to study Hall effects and heat transfer effects on the flow to be able to determine the efficiency of some devices such as power generators and heat exchanger. Attia [10] examined the unsteady Hartmann flow with heat transfer of a viscoelastic fluid considering Hall effect. Asghar *et al.*, [11] studied the effects of Hall current and heat transfer on flow due to a pull of eccentric rotating disk. Hayat *et al.*, [12] analyzed the Hall effects on peristaltic flow of Maxwell fluid in a porous medium. Abo-Eldahab *et al.*, [13-14] investigated the effects of Hall and ion-slip current on magnetohydrodynamic peristaltic transport and couple stress fluid.

When heat and mass transfer occur simultaneously in a moving fluid, the relations between the fluxes and the driving potentials are of more intricate nature. It has been found that an energy flux can be generated not only by temperature gradients but also by composition gradients. The energy

flux caused by a composition gradient is called Dufour or diffusion thermo effect [15]. On the other hand, mass fluxes can also be created by temperature gradients and this is Soret or thermal-diffusion effect. In general, Soret and Dufour effects have an order of magnitude which is smaller than the effects described in Fourier's or Fick's law and are often neglected in heat and mass transfer processes. Though these effects are quite small, certain devices can be arranged to produce very steep temperature and concentration gradients so that the separation of components in mixtures are affected. However, exceptions are observed therein. Due to the importance of Soret (thermal-diffusion) and Dufour (diffusion-thermo) effects for the fluids with very light molecular weight as well as medium molecular weight, many investigators have studied and reported results for these flows [16-18]. Heat and mass transfer effects on radially varying magnetic field of peristaltic motion of a non-Newtonian fluid was analyzed by El-dabe and Abouzeid [19]. Effects of heat and mass transfer on MHD peristaltic flow of a non-Newtonian nanofluid with couple stresses are discussed by Abouzeid [20]. El-dabe *et al.*, [21] studied Eyring-Powell nanofluid flow problem with gyrotactic microorganisms through the boundary layer in the presence of thermal diffusion and diffusion thermo effects. A variety of analysis have been presented heat and mass transfer problems keeping different flow geometries and fluid models [22-24].

In the present paper, we shall extend the work of Mekheimer *et al.*, [4] to include the non-Newtonian (Casson model), Hall current effects, porous medium, mass transfer, radiation, thermo-diffusion and diffusion-thermo effects, chemical reaction through a horizontal annulus. Explicit finite difference technique is used to solve the momentum, heat, and concentration equations. The axial velocity, temperature and concentration distributions are obtained as a function of the fluid properties. The effects of various parameters on these solutions are discussed and illustrated graphically through a set of figures.

2. Mathematical Formulations

Consider the peristaltic flow of an incompressible electrically conducting non-Newtonian fluid obeying Casson model with heat and mass transfer between two coaxial tubes. The flow is through a porous medium and in the presence of a strong magnetic cross-field producing the effect of Hall current. We use cylindrical coordinates system (R', θ, Z') where R' is the radial direction, Z' lies along the center line of the inner and outer tubes, the geometry of the wall surfaces is described in (Figure 1).

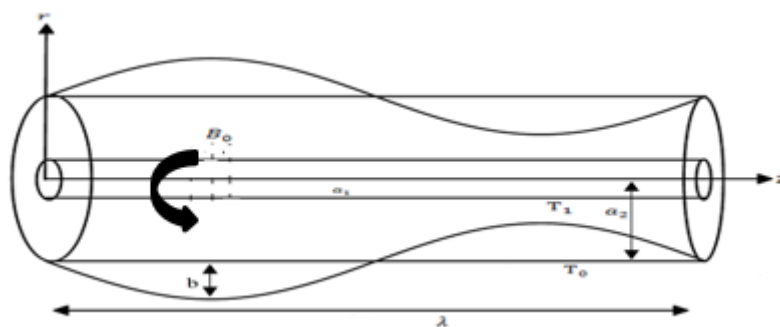


Fig. 1. Geometry of the problem

The equation of radii can be written as [25]

$$R'_1 = a_1 \tag{1}$$

$$R'_2 = a_2 + b \cos \frac{2\pi}{\lambda} (Z' - ct') \quad (2)$$

3. Basic Equations

The equations that govern the flow are given by

The continuity equation

$$\frac{\partial \rho}{\partial t} + \rho \nabla \cdot \underline{V} = 0 \quad (3)$$

The momentum equation

$$\rho \left(\frac{\partial \underline{V}}{\partial t} + \underline{V} \cdot \nabla \underline{V} \right) = -\nabla P + \nabla \cdot \underline{\tau} - \frac{\mu_\beta}{k_p} \underline{V} + \underline{J} \wedge \underline{B} \quad (4)$$

Ohm's law may be put in the form by taking Hall effects into account

$$\underline{J} = \frac{\sigma}{(1 + m^2)} (\underline{V} \wedge \underline{B} - \beta \underline{J} \wedge \underline{B}) \quad (m \text{ is Hall parameter}) \quad (5)$$

The energy equation

$$\rho C_p \left(\frac{\partial T}{\partial t} + \underline{V} \cdot \nabla T \right) = k_c \nabla^2 T + Q_0 + \Gamma_{ij} \frac{\partial V_i}{\partial x_j} + \frac{\rho D_m k_T}{C_s} \nabla^2 C \quad (6)$$

The concentration equation

$$\left(\frac{\partial C}{\partial t} + \underline{V} \cdot \nabla C \right) = D_m \nabla^2 C - A(C - C_\infty) + \frac{D_m k_T}{T_m} \nabla^2 T \quad (7)$$

The Casson (biviscosity) model can be written as

$$\tau_{ij} = \begin{cases} 2(\mu_\beta + P_y/\sqrt{2\pi})e_{ij} & \pi > \pi_c \\ 2(\mu_\beta + P_y/\sqrt{2\pi_c})e_{ij} & \pi < \pi_c \end{cases} \quad (8)$$

For ordinary Newtonian fluid, the yielding stress ($P_y = 0$). Since the flow parameter are independent of the azimuthal coordinate θ , then for the unsteady two-dimensional flow, the velocity components are given by

$$\underline{V} = (U', 0, W') \quad (9)$$

and the imposed magnetic field is $\underline{B} = (0, B_0, 0)$. Also, the temperature and the concentration distributions may be written as follows,

$$T = T(R', Z') \quad \text{and} \quad C = C(R', Z') \quad (10)$$

From Eq. (5) and (8), the governing equations in Eq. (4), (6) and (7) become

$$\frac{\partial U'}{\partial R'} + \frac{U'}{R'} + \frac{\partial W'}{\partial Z'} = 0 \quad (11)$$

$$\rho \left(\frac{\partial U'}{\partial t'} + U' \frac{\partial U'}{\partial R'} + W' \frac{\partial U'}{\partial Z'} \right) = - \frac{\partial P'}{\partial R'} + \frac{\partial \tau'_{RR}}{\partial R'} + \frac{\partial \tau'_{RZ}}{\partial Z'} + \frac{\tau'_{RR}}{R'} - \frac{\tau'_{\theta\theta}}{R'} - \frac{\sigma B_0^2}{1+m^2} (U' + mW') - \frac{\mu_\beta}{k_p} U' \quad (12)$$

$$\rho \left(\frac{\partial W'}{\partial t'} + U' \frac{\partial W'}{\partial R'} + W' \frac{\partial W'}{\partial Z'} \right) = - \frac{\partial P'}{\partial Z'} + \frac{\partial \tau'_{ZZ}}{\partial Z'} + \frac{\partial \tau'_{RZ}}{\partial R'} + \frac{\tau'_{RZ}}{R'} - \frac{\sigma B_0^2}{1+m^2} (W' - mU') - \frac{\mu_\beta}{k_p} W' \quad (13)$$

$$\rho C_p \left(\frac{\partial T'}{\partial t'} + U' \frac{\partial T'}{\partial R'} + W' \frac{\partial T'}{\partial Z'} \right) = K_c \left(\frac{\partial^2 T'}{\partial R'^2} + \frac{1}{R} \frac{\partial T'}{\partial R'} + \frac{\partial^2 T'}{\partial Z'^2} \right) + \tau'_{ZZ} \frac{\partial W'}{\partial Z'} + \tau'_{RZ} \frac{\partial U'}{\partial Z'} + \tau'_{RR} \frac{\partial U'}{\partial R'} + \tau'_{ZR} \frac{\partial W'}{\partial R'} - \frac{1}{R'} \frac{\partial (R' q_r)}{\partial R'} + Q_0 + \frac{\rho D_m k_T}{C_s} \left(\frac{\partial^2 C'}{\partial R'^2} + \frac{1}{R} \frac{\partial C'}{\partial R'} + \frac{\partial^2 C'}{\partial Z'^2} \right) \quad (14)$$

$$\left(\frac{\partial C'}{\partial t'} + U' \frac{\partial C'}{\partial R'} + W' \frac{\partial C'}{\partial Z'} \right) = D_m \left(\frac{\partial^2 C'}{\partial R'^2} + \frac{1}{R} \frac{\partial C'}{\partial R'} + \frac{\partial^2 C'}{\partial Z'^2} \right) - A(C - C_\infty) + \frac{D_m k_T}{T_m} \left(\frac{\partial^2 T'}{\partial R'^2} + \frac{1}{R} \frac{\partial T'}{\partial R'} + \frac{\partial^2 T'}{\partial Z'^2} \right) \quad (15)$$

where

$$\left. \begin{aligned} \tau'_{RR} &= 2\mu_\beta (1 + \gamma^{-1}) \frac{\partial U'}{\partial R'} \\ \tau'_{\theta\theta} &= 2\mu_\beta (1 + \gamma^{-1}) \frac{U'}{R'} \\ \tau'_{Rz} &= \mu_\beta (1 + \gamma^{-1}) \left(\frac{\partial U'}{\partial Z'} + \frac{\partial W'}{\partial R'} \right) \\ \tau'_{ZZ} &= 2\mu_\beta (1 + \gamma^{-1}) \frac{\partial W'}{\partial Z'} \end{aligned} \right\} \quad (16)$$

We shall consider the following transformation

$$z' = Z' - ct', \quad r' = R' \quad (17)$$

The velocities in the fixed and moving frames are related by

$$w' = W' - c, \quad u' = U', \quad p' = P'(z', t') \quad (18)$$

After using these transformations and Eq. (16), the equations of motion become

$$\frac{\partial u'}{\partial r'} + \frac{u'}{r'} + \frac{\partial w'}{\partial z'} = 0 \quad (19)$$

$$\begin{aligned} \rho \left(u' \frac{\partial u'}{\partial r'} + w' \frac{\partial u'}{\partial z'} \right) = & - \frac{\partial p'}{\partial r'} + \mu_\beta (1 + \gamma^{-1}) \left(\frac{\partial^2 u'}{\partial r'^2} + \frac{1}{r'} \frac{\partial u'}{\partial r'} + \frac{\partial^2 u'}{\partial z'^2} - \frac{u'}{r'^2} \right) \\ & - \frac{\sigma B_0^2}{1 + m^2} (u' + m(w' + c)) - \frac{\mu_\beta}{k_p} u' \end{aligned} \quad (20)$$

$$\begin{aligned} \rho \left(u' \frac{\partial w'}{\partial r'} + w' \frac{\partial w'}{\partial z'} \right) = & - \frac{\partial p'}{\partial z'} + \mu_\beta (1 + \gamma^{-1}) \left(\frac{\partial^2 w'}{\partial r'^2} + \frac{1}{r'} \frac{\partial w'}{\partial r'} + \frac{\partial^2 w'}{\partial z'^2} \right) \\ & - \frac{\sigma B_0^2}{1 + m^2} ((w' + c) - mu') - \frac{\mu_\beta}{k_p} w' \end{aligned} \quad (21)$$

$$\begin{aligned} \rho C_p \left(u \frac{\partial T'}{\partial r'} + w' \frac{\partial T'}{\partial z'} \right) = & k_c \left(\frac{\partial^2 T'}{\partial r'^2} + \frac{1}{r'} \frac{\partial T'}{\partial r'} + \frac{\partial^2 T'}{\partial z'^2} \right) + \frac{3R}{4} \left(\frac{\partial^2 T'}{\partial r'^2} + \frac{1}{r'} \frac{\partial T'}{\partial r'} \right) \\ & + \mu_\beta (1 + \gamma^{-1}) \left[2 \left(\frac{\partial u'}{\partial r'} \right)^2 + 2 \left(\frac{\partial w'}{\partial z'} \right)^2 + \left(\frac{\partial u'}{\partial z'} + \frac{\partial w'}{\partial r'} \right)^2 \right] \\ & + Q_0 + \frac{\rho D_m k_T}{C_s} \left(\frac{\partial^2 C'}{\partial r'^2} + \frac{1}{r'} \frac{\partial C'}{\partial r'} + \frac{\partial^2 C'}{\partial z'^2} \right) \end{aligned} \quad (22)$$

$$\begin{aligned} \left(u' \frac{\partial C'}{\partial r'} + w' \frac{\partial C'}{\partial z'} \right) = & D_m \left(\frac{\partial^2 C'}{\partial r'^2} + \frac{1}{r'} \frac{\partial C'}{\partial r'} + \frac{\partial^2 C'}{\partial z'^2} \right) - A(C' - C_\infty) \\ & + \frac{D_m k_T}{T_m} \left(\frac{\partial^2 T'}{\partial r'^2} + \frac{1}{r'} \frac{\partial T'}{\partial r'} + \frac{\partial^2 T'}{\partial z'^2} \right) \end{aligned} \quad (23)$$

The appropriate boundary conditions are given by

$$\left. \begin{aligned} u' = 0, \quad w' = 0, \quad T' = 0, \quad C' = 0 \quad \text{at} \quad r = r_1' \\ u' = -c \frac{\partial R_2'}{\partial z'}, \quad w' = -c, \quad T' = T_1, \quad C' = C_1 \quad \text{at} \quad r = r_2' \end{aligned} \right\} \quad (24)$$

The appropriate non-dimensional variable for the flow are defined as

$$\left. \begin{aligned} r^* &= \frac{r'}{a_2}, \quad z^* = \frac{z'}{\lambda}, \quad u^* = \frac{\lambda}{ca_2}u', \quad w^* = \frac{w'}{c}, \quad P^* = \frac{a_2^2}{c\lambda\mu}P, \quad t^* = \frac{c}{\lambda}t' \\ \theta^* &= \frac{T' - T_0}{T_1 - T_0}, \quad \phi^* = \frac{C' - C_0}{C_1 - C_0}, \quad r_2^* = \frac{R_2'}{a_2}, \quad \delta = \frac{a_2}{\lambda}, \quad Re = \frac{\rho ca_2}{\mu}, \quad \varepsilon = \frac{b}{a_2} \end{aligned} \right\} \quad (25)$$

In terms of these variables and dropping the star mark for simplicity, Eq. (19)-(23) become

$$\frac{1}{r} \frac{\partial(ru)}{\partial r} + \frac{\partial w}{\partial z} = 0 \quad (26)$$

$$\begin{aligned} Re \delta^3 \left(u \frac{\partial u}{\partial r} + w \frac{\partial u}{\partial z} \right) &= -\frac{\partial P}{\partial r} + \delta^2 (1 + \gamma^{-1}) \left(\frac{\partial^2 u}{\partial r^2} + \frac{1}{r} \frac{\partial u}{\partial r} + \delta^2 \frac{\partial^2 u}{\partial z^2} - \frac{u}{r^2} \right) \\ &\quad - \delta^2 \frac{1}{Da} u - \frac{\delta M}{(1 + m^2)} (\delta u + m(w + 1)) \end{aligned} \quad (27)$$

$$\begin{aligned} Re \delta \left(u \frac{\partial w}{\partial r} + w \frac{\partial w}{\partial z} \right) &= -\frac{\partial P}{\partial z} + (1 + \gamma^{-1}) \left(\frac{\partial^2 w}{\partial r^2} + \frac{1}{r} \frac{\partial w}{\partial r} + \delta^2 \frac{\partial^2 w}{\partial z^2} \right) \\ &\quad - \frac{1}{Da} w - \frac{M}{(1 + m^2)} ((w + 1) - m\delta u) \end{aligned} \quad (28)$$

$$\begin{aligned} Re \delta Pr \left(u \frac{\partial \theta}{\partial r} + w \frac{\partial \theta}{\partial z} \right) &= \left(1 + \frac{4R}{3} \right) \left(\frac{\partial^2 \theta}{\partial r^2} + \frac{1}{r} \frac{\partial \theta}{\partial r} \right) + \delta^2 \frac{\partial^2 \theta}{\partial z^2} \\ &\quad + Ec (1 + \gamma^{-1}) \left(2\delta^2 \left(\frac{\partial u}{\partial r} \right)^2 + 2\delta^2 \left(\frac{\partial w}{\partial z} \right)^2 + \left(\delta^2 \frac{\partial u}{\partial z} + \frac{\partial w}{\partial r} \right)^2 \right) \\ &\quad + \beta + Df \left(\frac{\partial^2 \phi}{\partial r^2} + \frac{1}{r} \frac{\partial \phi}{\partial r} + \delta^2 \frac{\partial^2 \phi}{\partial z^2} \right) \end{aligned} \quad (29)$$

$$\begin{aligned} Re \delta Sc \left(u \frac{\partial \phi}{\partial r} + w \frac{\partial \phi}{\partial z} \right) &= \left(\frac{\partial^2 \phi}{\partial r^2} + \frac{1}{r} \frac{\partial \phi}{\partial r} + \delta^2 \frac{\partial^2 \phi}{\partial z^2} \right) - L\phi Sc \\ &\quad + Sc Sr \left(\frac{\partial^2 \theta}{\partial r^2} + \frac{1}{r} \frac{\partial \theta}{\partial r} + \delta^2 \frac{\partial^2 \theta}{\partial z^2} \right) \end{aligned} \quad (30)$$

The radii equations become

$$\left. \begin{aligned} r_1 &= \frac{a_1}{a_2} \\ r_2 &= 1 + \varepsilon \cos 2\pi z \end{aligned} \right\} \quad (31)$$

Also, the boundary conditions in Eq. (24) in their dimensionless form read

$$\left. \begin{aligned} u = 0, \quad w = 0, \quad \theta = 0, \quad \varphi = 0 \quad \text{at} \quad r_1 = \frac{1}{2} \\ u = -\frac{\partial r_2}{\partial z} \quad w = -1, \quad \theta = 1, \quad \varphi = 1 \quad \text{at} \quad r_2 = 1 + \varepsilon \cos 2\pi z \end{aligned} \right\} \quad (32)$$

Using the long wavelength approximation and dropping terms of order δ and higher, then Eq. (27)-(30) take the following form

$$0 = -\frac{\partial P}{\partial r} \quad (33)$$

$$0 = -\frac{\partial P}{\partial z} + (1 + \gamma^{-1}) \left(\frac{\partial^2 w}{\partial r^2} + \frac{1}{r} \frac{\partial w}{\partial r} \right) - \frac{1}{Da} w - \frac{M}{(1 + m^2)} (w + 1) \quad (34)$$

$$\left(1 + \frac{4R}{3}\right) \left(\frac{\partial^2 \theta}{\partial r^2} + \frac{1}{r} \frac{\partial \theta}{\partial r} \right) + Pr\beta + PrDf \left(\frac{\partial^2 \varphi}{\partial r^2} + \frac{1}{r} \frac{\partial \varphi}{\partial r} \right) + PrEc (1 + \gamma^{-1}) \left(\frac{\partial w}{\partial r} \right)^2 = 0 \quad (35)$$

$$\frac{\partial^2 \varphi}{\partial r^2} + \frac{1}{r} \frac{\partial \varphi}{\partial r} + ScSr \left(\frac{\partial^2 \theta}{\partial r^2} + \frac{1}{r} \frac{\partial \theta}{\partial r} \right) - ScL\varphi = 0 \quad (36)$$

Eq. (33) indicates that P depends on z only. The Eq. (34)-(36) subjected to boundary conditions (32) are solved numerically by using the semi-discretization finite difference method which is known as method of lines [26]. Spatial interval $0.5 \leq r \leq r_2$ is partitioned into N equal parts with grid size $\Delta r = 1/N$ and grid points $r_i = (i - 1) \Delta r$, $1 \leq i \leq N + 1$. The first and second spatial derivatives in Eq. (34)-(36) are approximated with second-order central finite differences, then a Newton iteration method is used until either the specified accuracy goal or precision goal is achieved.

In the case of ordinary Newtonian fluid ($P_y = 0$), for non-porous medium $\frac{1}{Da} \rightarrow 0$, in the absence of radiation, viscous dissipation effects and when the concentration equation is not taken into consideration, the system of above equations will reduce to Mekheimer and Abd-elmaboud [4].

4. Results and Discussion

The effects of various parameters involved in the problem such as magnetic parameter (Hartman number) M , the upper limit apparent viscosity coefficient γ , Hall parameter m , the pressure gradient dp/dz , Prandtl number Pr , Eckert number Ec , Darcy number Da , Dufour number Df , the radiation parameter N , Schmidt number Sc , Soret number Sr , the chemical reaction parameter L and heat source/sink parameter β , on the axial velocity w , the temperature θ and the concentration φ are discussed in the Figure 2-19.

The effects of physical parameters on the axial velocity w are indicated through Figure 2-4. In these figures the axial velocity w is plotted versus the radial coordinate r . In Figure 2 and 3, the effects of the pressure gradient dp/dz and (Hartman number) M on the axial velocity w are presented. It is seen from these figures that the velocity is always negative, and it decreases by increasing both dp/dz and M values. The obtained result in Figure 3 is due to the Lorentz force which

retards the flow. Similarly, if we draw the variation of w with r for different values of Darcy number Da and the upper limit apparent viscosity coefficient γ , we will obtain a figures in which the behavior of the curves are the same as that obtained in Figure 2 and 3 except that the obtained curves are very closed to those obtained in Figure 2 and 3. Figure 4 shows the variation of the axial velocity w with r for different values of Hall parameter m . It is observed that the axial velocity is always negative, and it increases by increasing m values, whereas it decreases by increasing r values.

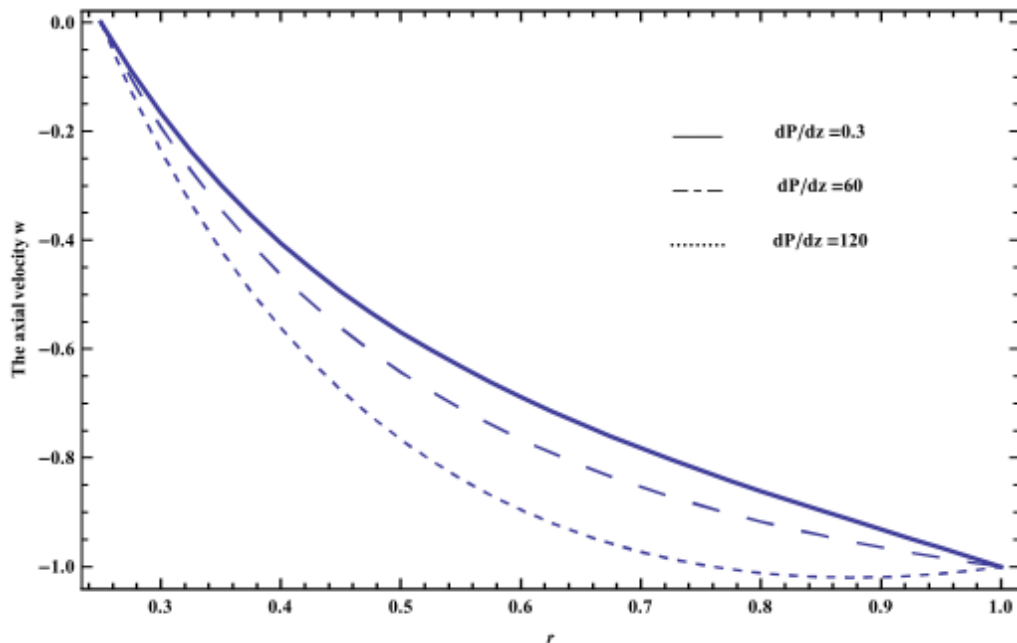


Fig. 2. The axial velocity is plotted versus r , for different values of dp/dz and for a system which has the particular values $M=100$, $\gamma=0.5$, $m=1.5$, $Pr=0.59$, $Ec=1.5$, $Da=0.05$, $Df=0.55$, $N=0.5$, $Sc=1$, $Sr=2$, $L=1.5$ and $\beta =0.4$

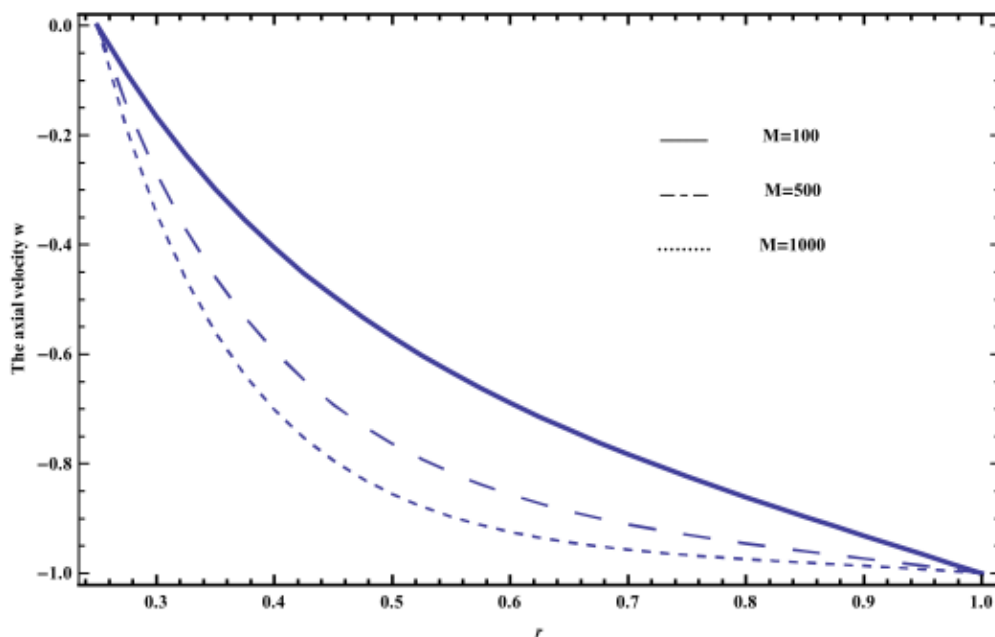


Fig. 3. The axial velocity is plotted versus r , for different values of M and for a system which has the particular values $\gamma=0.5$, $m=1.5$, $dp/dz=60$, $Pr=0.59$, $Ec=1.5$, $Da=0.05$, $Df=0.55$, $N=0.5$, $Sc=1$, $Sr=2$, $L=1.5$ and $\beta =0.4$

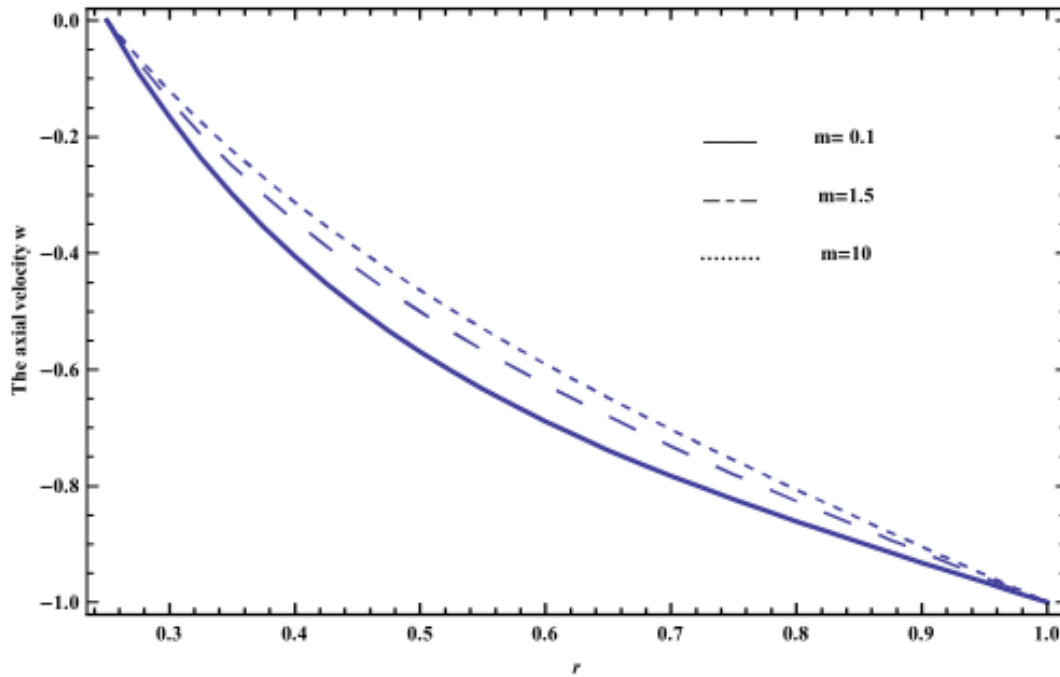


Fig. 4. The axial velocity is plotted versus r , for different values of m and for a system which has the particular values $M=100$, $\gamma=0.5$, $dp/dz=60$, $Pr=0.59$, $Ec=1.5$, $Da=0.05$, $Df=0.55$, $N=0.5$, $Sc=1$, $Sr=2$, $L=1.5$ and $\beta =0.4$

The effects of physical parameters on the temperature distribution θ are given through Figure 5-12. Figure 5 illustrates the effect of the pressure gradient dp/dz on the temperature distribution θ , and indicates that for a constant value of dp/dz , the variation of temperature distribution θ increases by increasing r till a maximum value (at a finite value of $r : r = r_0$) after which it decreases. Also, it is found from this figure that the temperature distribution θ increases by increasing the pressure gradient dp/dz when $r \in [0.23, 0.8]$, while it decreases afterwards. Figure 6 represents the behaviors of the temperature distribution θ with r for different values of (Hartman number) M . It is found that the temperature distribution θ increases with increase of M when $r \in [0.23, 0.58]$, while it decreases afterwards. Similar result to that shown in Figure 6 can be obtained if M is replaced by Darcy number Da except that the obtained curves are very closed to those obtained in Figure 6.

The effect of Hall parameter m on the temperature distribution θ is illustrated in Figure 7. It is noted that the temperature distribution θ decreases with increases of m when $r \in [0.23, 0.52]$, while it increases afterwards.

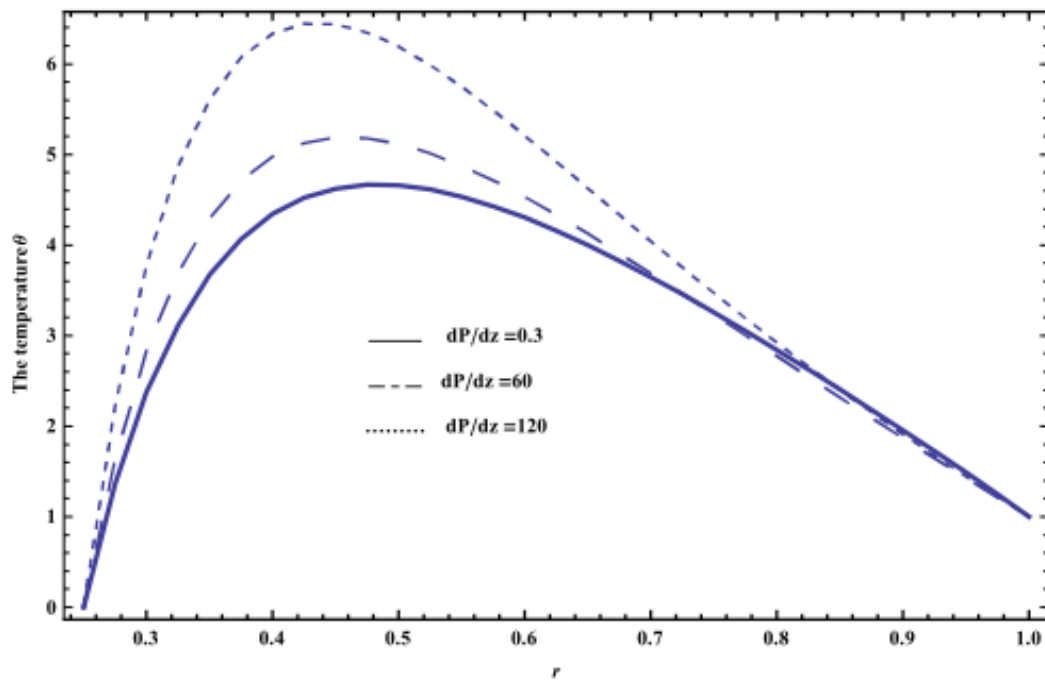


Fig. 5. The temperature is plotted versus r , for different values of dp/dz and for a system which has the particular values $M=100$, $\gamma=0.5$, $m=1.5$, $Pr=0.59$, $Ec=1.5$, $Da=0.05$, $Df=0.55$, $N=0.5$, $Sc=1$, $Sr=2$, $L=1.5$ and $\beta = 0.4$

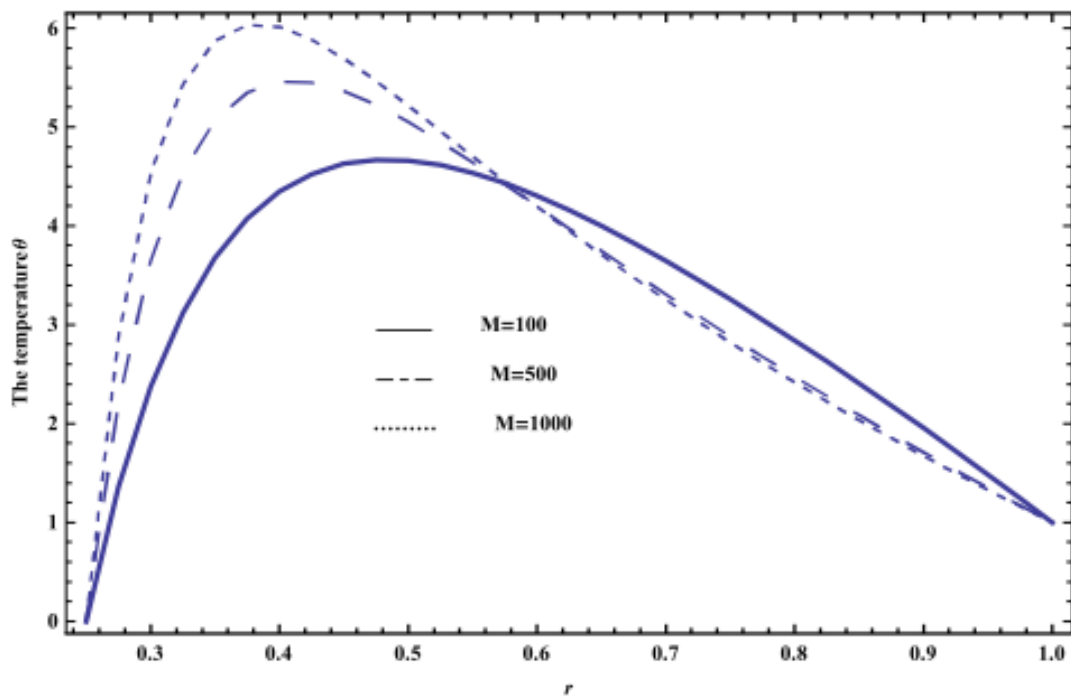


Fig. 6. The temperature is plotted versus r , for different values of M and for a system which has the particular values $\gamma=0.5$, $m=1.5$, $dp/dz=60$, $Pr=0.59$, $Ec=1.5$, $Da=0.05$, $Df=0.55$, $N=0.5$, $Sc=1$, $Sr=2$, $L=1.5$ and $\beta = 0.4$

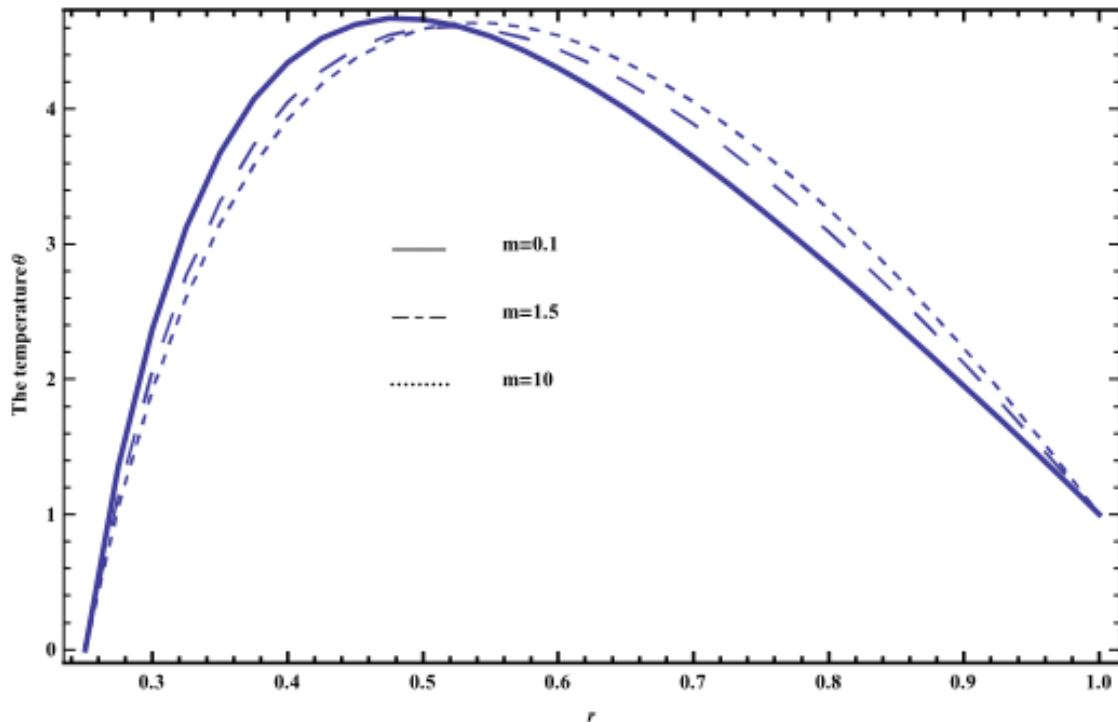


Fig. 7. The temperature is plotted versus r , for different values of m and for a system which has the particular values $M=100$, $\gamma=0.5$, $dp/dz=60$, $Pr=0.59$, $Ec=1.5$, $Da=0.05$, $Df=0.55$, $N=0.5$, $Sc=1$, $Sr=2$, $L=1.5$ and $\beta =0.4$

The temperature distribution θ with r for different values of heat source/sink parameter β and the radiation parameter N , respectively, are displayed in Figure 8 and 9, respectively. The graphical results of Figure 8 and 9 indicate that the temperature distribution θ increases with increasing in the parameter β , while it decreases by increasing the parameter N , respectively. The effect of Eckert number Ec and Soret number Sr on the temperature distribution θ are found to be similar to the effect of β given by Figure 8 except that the obtained curves are very closed to those obtained in Figure 8. Figure 10 and 11 illustrate the change of the temperature distribution θ versus r with several values of Dufour number Df and the upper limit apparent viscosity coefficient γ , respectively. It is seen, from Figure 10 and 11, the temperature distribution θ increases with increasing in the parameter Df , while it decreases by increasing the parameter γ , respectively. It is also noted that the difference of the temperature distribution θ for different values of Df and γ becomes greater with increasing the radial coordinate and reaches maximum value after which it decreases. The following explains the result in Figure 11. the upper limit apparent viscosity coefficient is proportional to the dynamic viscosity which is inversely proportionally to the fluid temperature. In Figure 12, the effect of Prandtl number Pr on the temperature distribution θ is illustrated. It is clear from this figure that the temperature distribution θ increases with increasing Pr . Similarly, if we draw the temperature distribution θ with r for different values of Schmidt number Sc , we will obtain a figures in which the behavior of the curves are the same as that obtained in Figure 12 except that the obtained curves are very closed to those obtained in Figure 12.

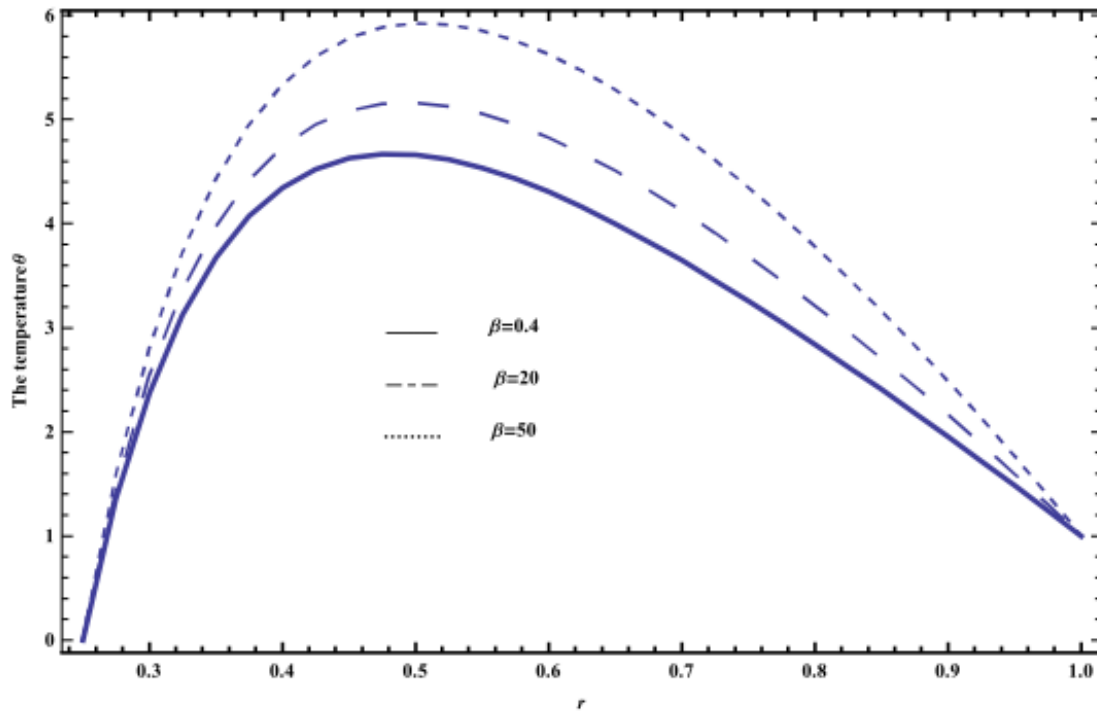


Fig. 8. The temperature is plotted versus r , for different values of β and for a system which has the particular values $M=100$, $\gamma=0.5$, $m=1.5$, $dp/dz=60$, $Pr=0.59$, $Ec=1.5$, $Da=0.05$, $Df=0.55$, $N=0.5$, $Sc=1$, $Sr=2$, and $L=1.5$

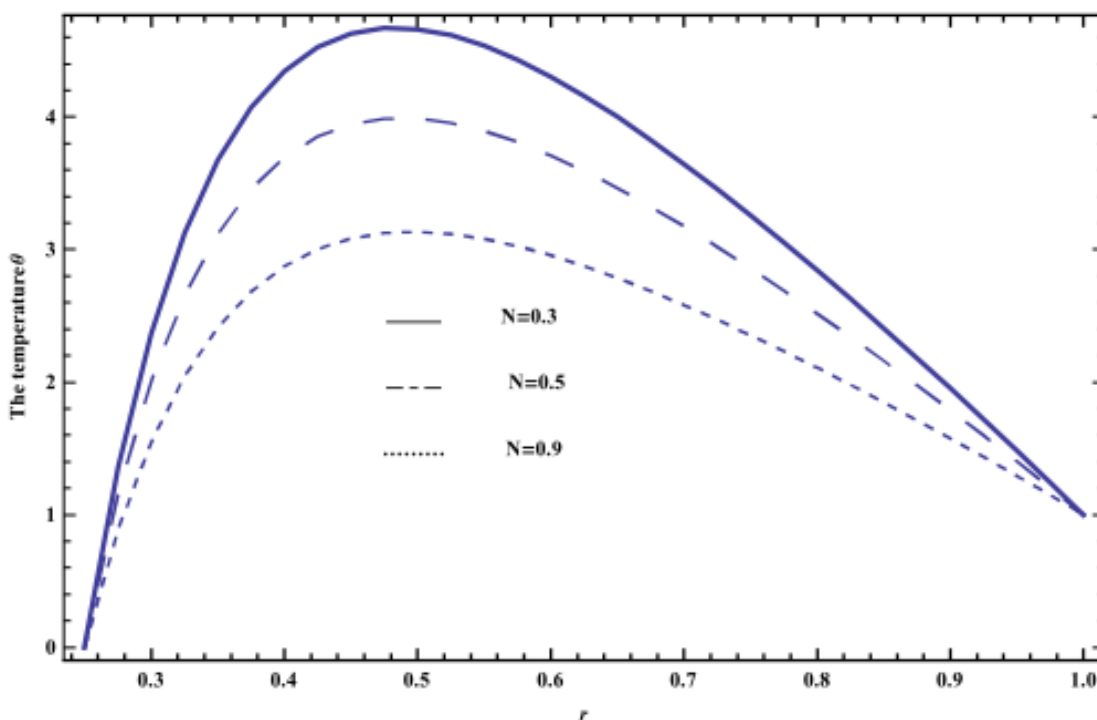


Fig. 9. The temperature is plotted versus r , for different values of N and for a system which has the particular values $M=100$, $\gamma=0.5$, $m=1.5$, $dp/dz=60$, $Pr=0.59$, $Ec=1.5$, $Da=0.05$, $Df=0.55$, $Sc=1$, $Sr=2$, $L=1.5$ and $\beta =0.4$

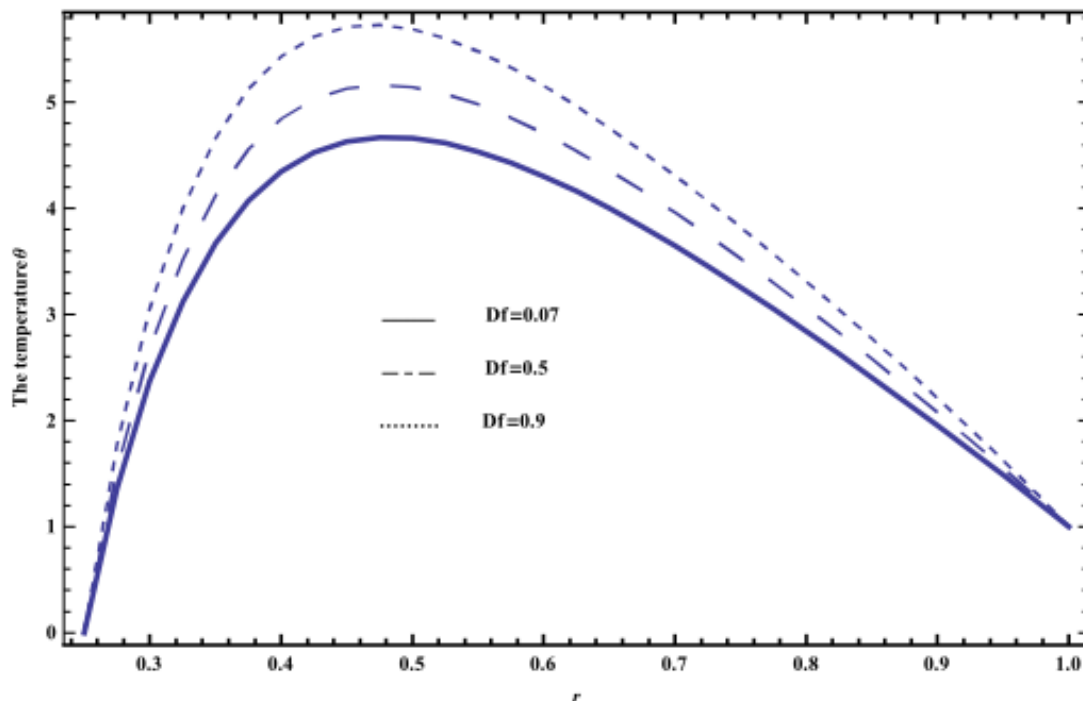


Fig. 10. The temperature is plotted versus r , for different values of Df and for a system which has the particular values $M=100$, $\gamma=0.5$, $m=1.5$, $dp/dz=60$, $Pr=0.59$, $Ec=1.5$, $Da=0.05$, $N=0.5$, $Sc=1$, $Sr=2$, $L=1.5$ and $\beta =0.4$

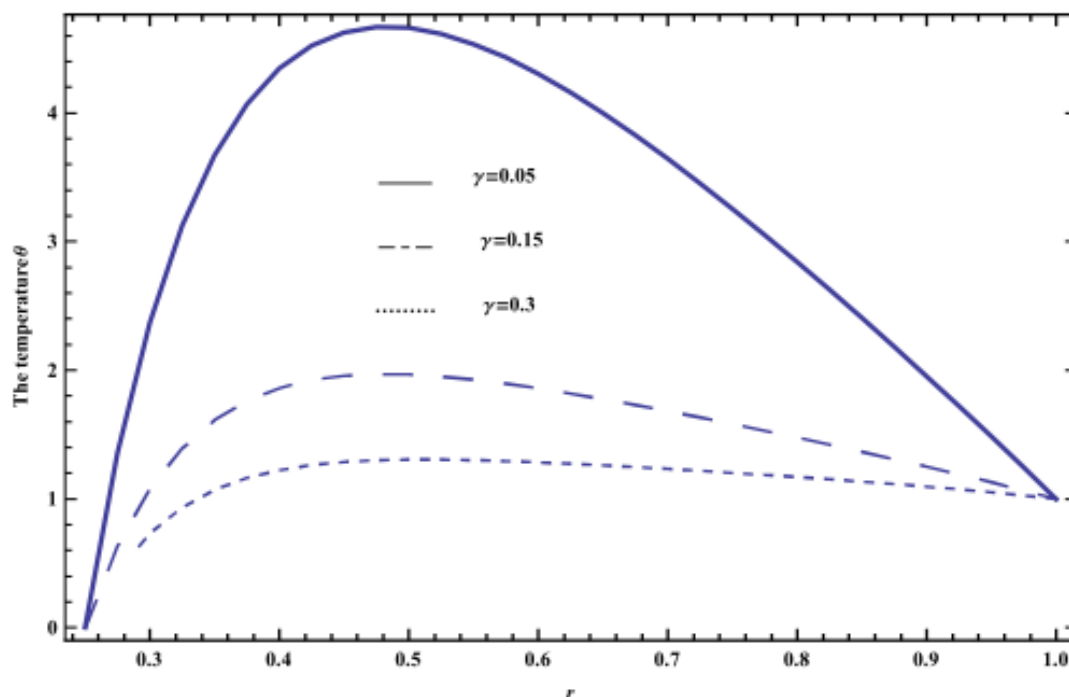


Fig. 11. The temperature is plotted versus r , for different values of γ and for a system which has the particular values $M=100$, $m=1.5$, $dp/dz=60$, $Pr=0.59$, $Ec=1.5$, $Da=0.05$, $Df=0.55$, $N=0.5$, $Sc=1$, $Sr=2$, $L=1.5$ and $\beta =0.4$

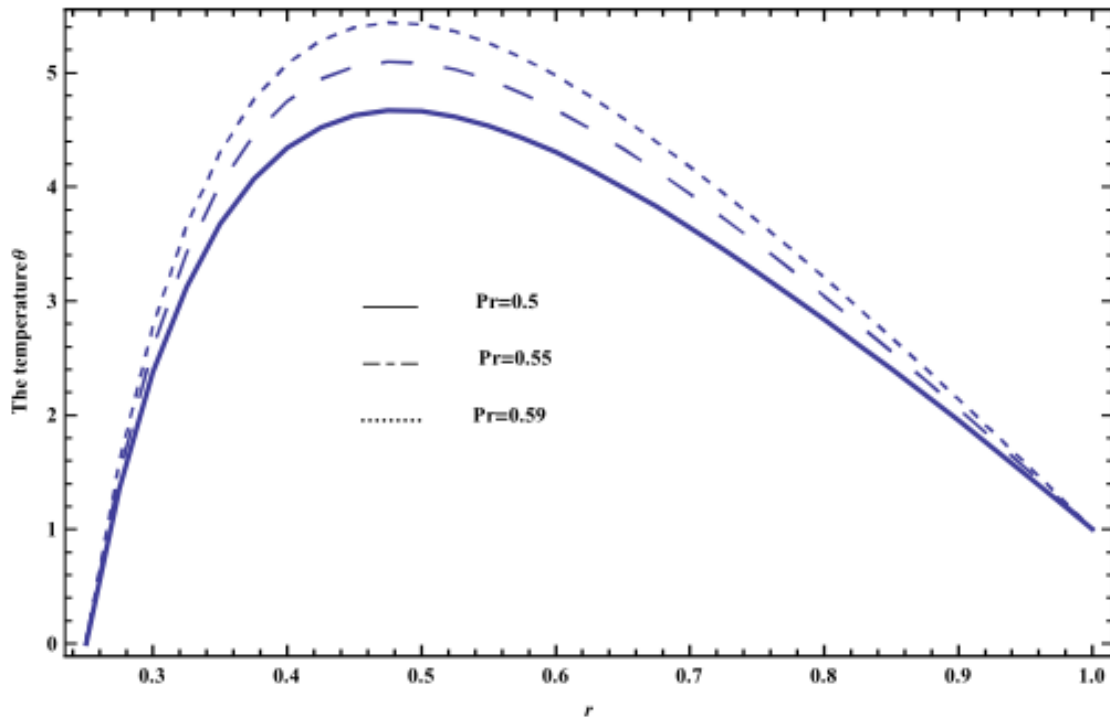


Fig. 12. The temperature is plotted versus r , for different values of Pr and for a system which has the particular values $M=100$, $\gamma=0.5$, $m=1.5$, $dp/dz=60$, $Pr=0.59$, $Ec=1.5$, $Da=0.05$, $Df=0.55$, $N=0.5$, $Sc=1$, $Sr=2$, $L=1.5$ and $\beta =0.4$

The effects of physical parameters on the concentration distribution ϕ indicated through Figure 13-19. In Figure 13 and 14, the effects of Hall parameter m and (Hartman number) M on the concentration distribution ϕ are indicated. It is seen from this figures that the concentration ϕ is always negative, and it increases by increasing m values when $r \in [0,0.54]$, while it decreases afterwards, whereas it decreases by increasing both of M and r values when $r \in [0,0.58]$, while it increases afterwards. Figure 15 illustrates the effect of the radiation parameter N on the concentration distribution ϕ . It is found that the concentration distribution ϕ is always negative, and it increases by increasing N values, whereas it decreases by increasing r values. Similarly, if we draw the concentration distribution ϕ with r for different values of the chemical reaction parameter L , we will obtain a figures in which the behavior of the curves are the same as that obtained in Figure 15 except that the obtained curves are very closed to those obtained in Figure 15. The concentration distribution ϕ with r for different values of Soret number Sr is displayed in Figure 16. The graphical results of Figure 16 indicates that the concentration distribution ϕ is always negative and it decreases with increasing both of Sr and r values. Similar result can be obtained as in Figure 16 by drawing the concentration distribution ϕ versus r for various values of Schmidt number Sc . Figure 17 shows the concentration distribution ϕ with r for various values of the pressure gradient dp/dz . From this figure, we observed that the concentration distribution ϕ is always negative and it decreases with increasing dp/dz when $r \in [0,0.7]$, while it increases afterwards, whereas it decreases by increasing r values. Similarly, if we draw the concentration distribution ϕ with r for different values of Darcy number Da , we will obtain a figures in which the behavior of the curves are the same as that obtained in Figure 17 except that the obtained curves are very closed to those obtained in Figure 17 and the concentration distribution ϕ decreases with increasing Da when $r \in [0,0.56]$.

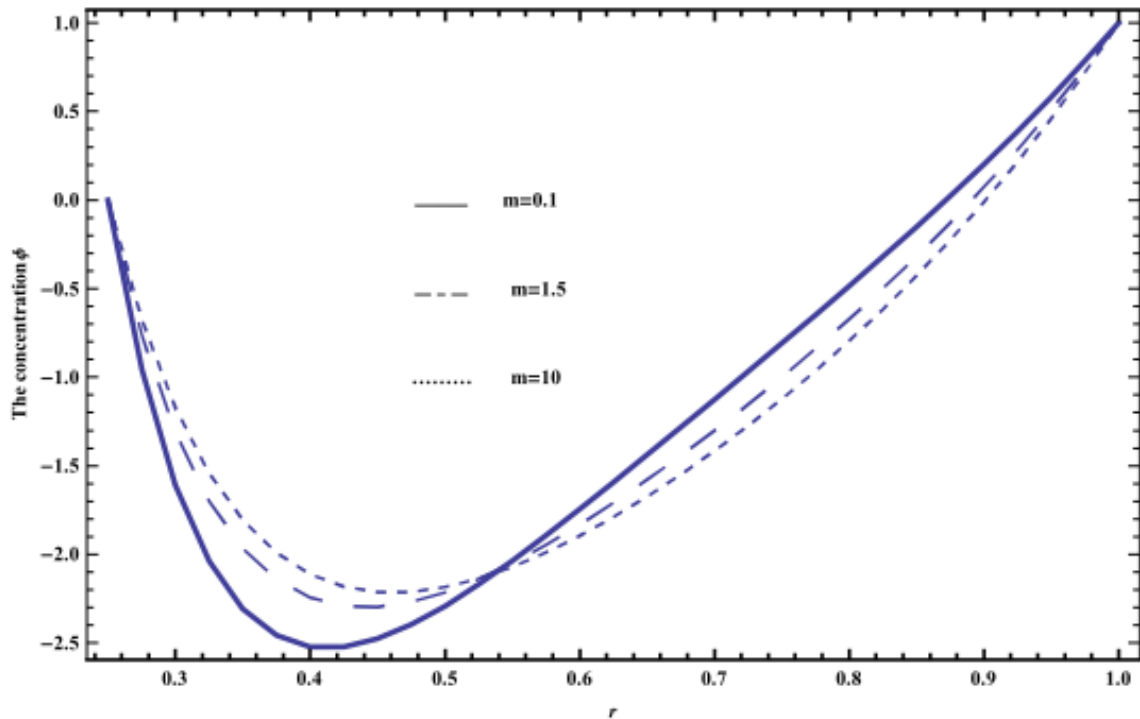


Fig. 13. The concentration is plotted versus r , for different values of m and for a system which has the particular values $M=100$, $\gamma=0.5$, $dp/dz=60$, $Pr=0.59$, $Ec=1.5$, $Da=0.05$, $Df=0.55$, $N=0.5$, $Sc=1$, $Sr=2$, $L=1.5$ and $\beta =0.4$

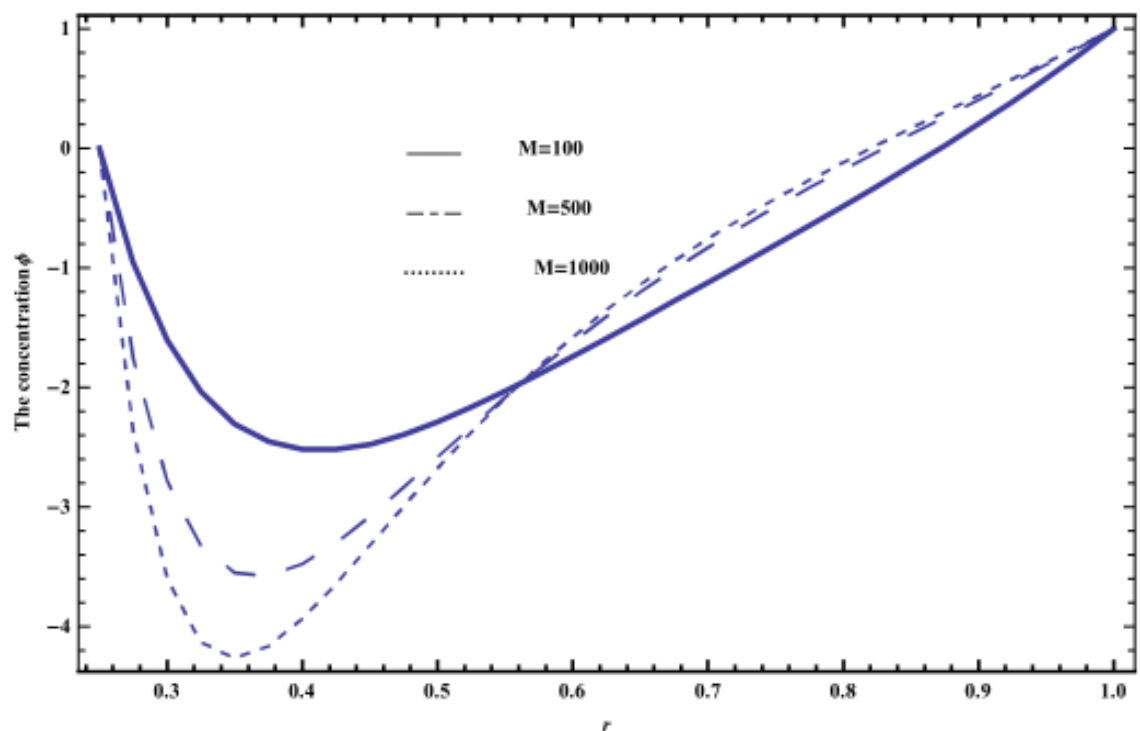


Fig. 14. The concentration is plotted versus r , for different values of M and for a system which has the particular values $\gamma=0.5$, $m=1.5$, $dp/dz=60$, $Pr=0.59$, $Ec=1.5$, $Da=0.05$, $Df=0.55$, $N=0.5$, $Sc=1$, $Sr=2$, $L=1.5$ and $\beta =0.4$

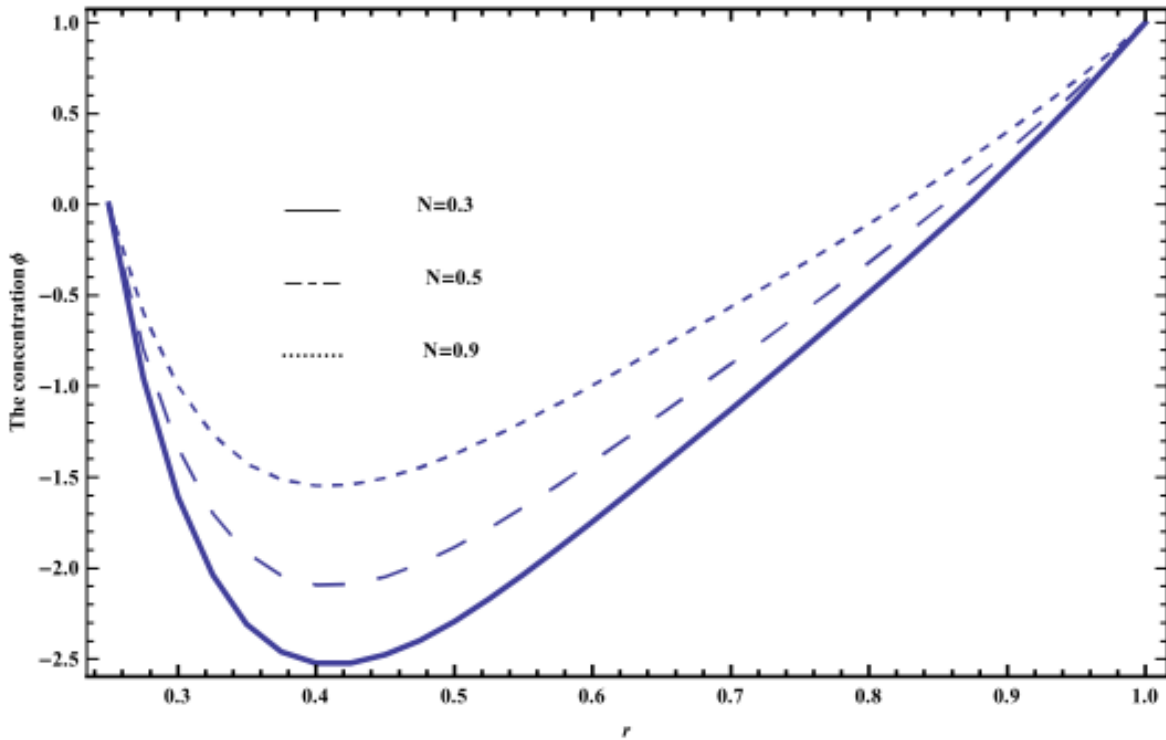


Fig. 15. The concentration is plotted versus r , for different values of N and for a system which has the particular values $M=100$, $\gamma=0.5$, $m=1.5$, $dp/dz=60$, $Pr=0.59$, $Ec=1.5$, $Da=0.05$, $Df=0.55$, $Sc=1$, $Sr=2$, $L=1.5$ and $\beta =0.4$

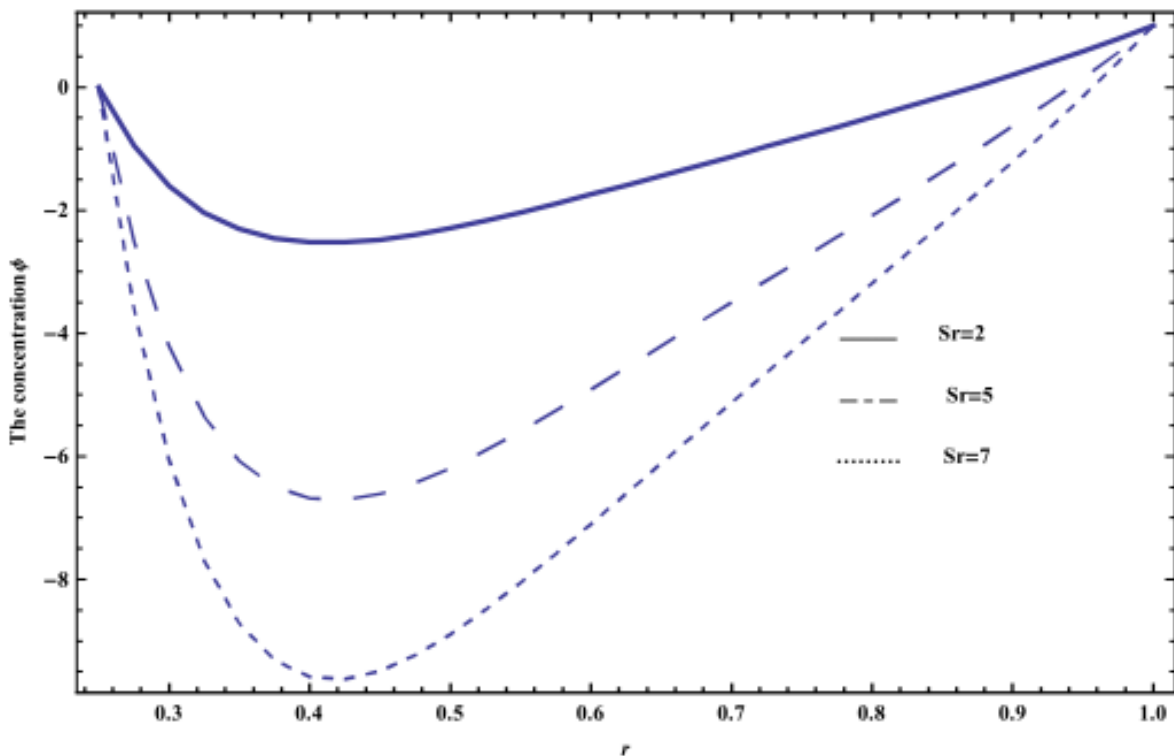


Fig. 16. The concentration is plotted versus r , for different values of Sr and for a system which has the particular values $M=100$, $\gamma=0.5$, $m=1.5$, $dp/dz=60$, $Pr=0.59$, $Ec=1.5$, $Da=0.05$, $Df=0.55$, $N=0.5$, $Sc=1$, $L=1.5$ and $\beta =0.4$

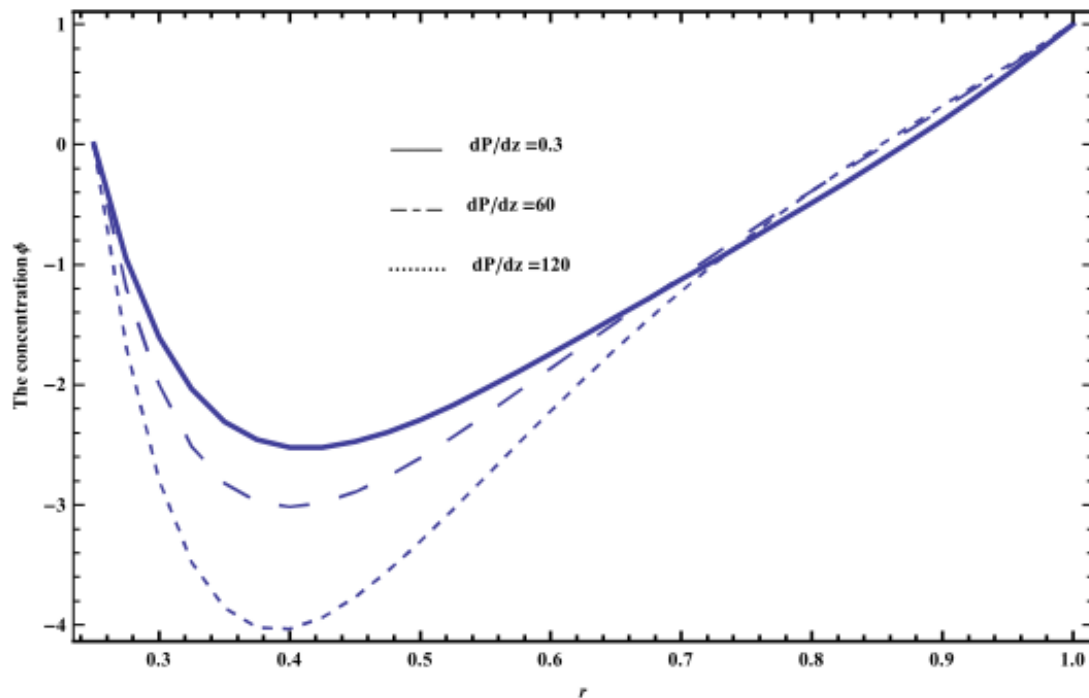


Fig. 17. The concentration is plotted versus r , for different values of dp/dz and for a system which has the particular values $M=100$, $\gamma=0.5$, $m=1.5$, $Pr=0.59$, $Ec=1.5$, $Da=0.05$, $Df=0.55$, $N=0.5$, $Sc=1$, $Sr=2$, $L=1.5$ and $\beta = 0.4$

The effect of heat source/sink parameter β on the concentration distribution ϕ is shown in Figure 18, it is clear that the concentration is always negative, and it decreases by increasing both β and r values.

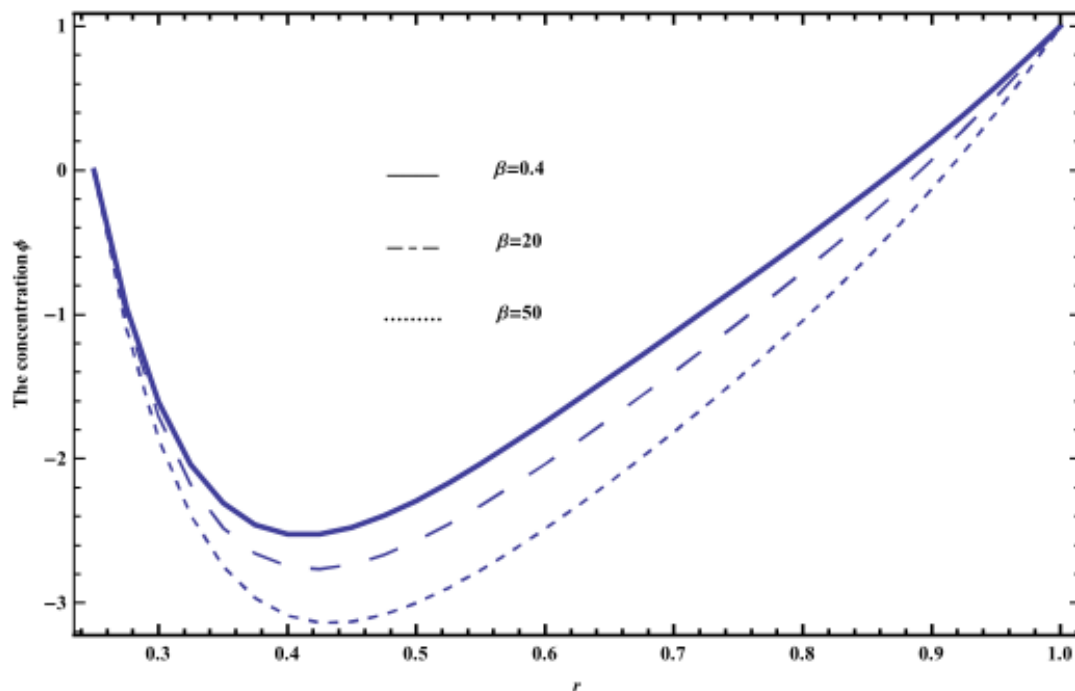


Fig. 18. The concentration is plotted versus r , for different values of β and for a system which has the particular values $M=100$, $\gamma=0.5$, $m=1.5$, $dp/dz=60$, $Pr=0.59$, $Ec=1.5$, $Da=0.05$, $Df=0.55$, $N=0.5$, $Sc=1$, $Sr=2$, and $L=1.5$

The effects of some parameters such Prandtl number Pr , Eckert number Ec and Dufour number Df , on the concentration distribution ϕ , respectively are found to be similar to the effect of β given in Figure 18 except that the obtained curves are very closed to those obtained in Figure 18. Finally, the concentration distribution ϕ with r for different values of the upper limit apparent viscosity coefficient γ is illustrated in Figure 19. It is observed that the concentration distribution ϕ is always negative and it increases by increasing γ values, whereas it decreases by increasing r values.

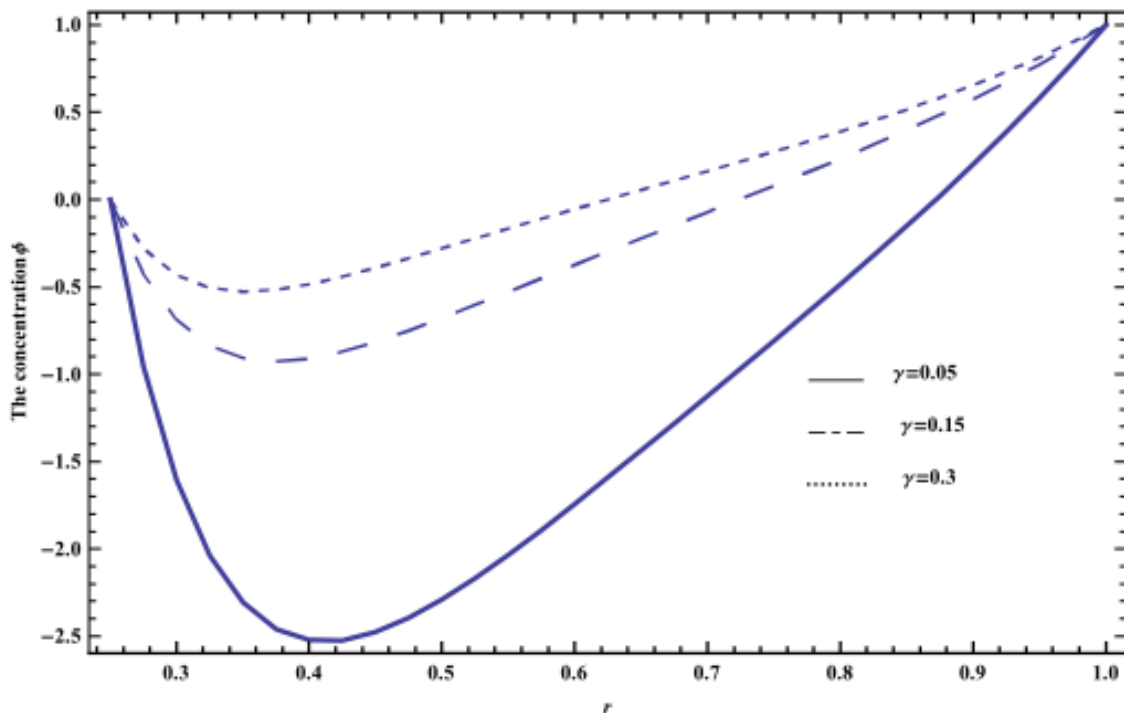


Fig. 19. The concentration is plotted versus r , for different values of γ and for a system which has the particular values $M=100$, $m=1.5$, $dp/dz=60$, $Pr=0.59$, $Ec=1.5$, $Da=0.05$, $Df=0.55$, $N=0.5$, $Sc=1$, $Sr=2$, $L=1.5$ and $\beta =0.4$

5. Conclusions

In this paper, we have studied the effects of radiation with hall current on unsteady flow of an incompressible non-Newtonian fluid through porous medium. The thermal-diffusion and diffusion thermo effects are taken to our consideration. The governing equations were solved numerically by using Mathematica after the condition of long wavelength with small Reynolds number were applied. We think that this paper deals with an important branch of fluid mechanics which has many important applications in many fields [27].

Peristaltic pumps are typically used to pump clean/sterile or aggressive fluids because cross contamination with exposed pump components cannot occur. Some common applications include pumping fluids through an infusion device, aggressive chemicals, high solids slurries and other materials where isolation of the product from the environment, and the environment from the product, are critical. It is also used in heart-lung machines to circulate blood during a bypass surgery as the pump does not cause significant hemolytic. Peristaltic pumps are also used in a wide variety of industrial applications. Their unique design makes them especially suited to pumping abrasives and viscous fluids. Moreover, Thermal-diffusion and diffusion-thermo effects is useful in various

scientific fields such as molecular and convective transport of particles, water evaporation, the chemical contamination diffusion in rivers and oceans etc.

The effects of various parameters of the problem on the velocity, temperature and concentration distributions are obtained and depicted graphically through a set of figures and the main results can be concluded as

- i. The axial velocity w increases with increase Hall parameter m .
- ii. The axial velocity w decreases by increasing both the pressure gradient dp/dz , Hartman number M , the upper limit apparent viscosity coefficient γ and Darcy number Da .
- iii. The temperature θ increases when the Prantl number Pr , Dufour number Df , the Soret number Sr , the heat source sink β and the Eckert number Ec increase.
- iv. The temperature decreases when the upper limit apparent viscosity coefficient γ and the radiation parameter N increase.
- v. The concentration ϕ increases when the radiation parameter N , the chemical reaction parameter L and the upper limit apparent viscosity coefficient γ increase.
- vi. The concentration ϕ decreases when the Schmidt number Sc , the Prantl number Pr , Dufour number Df , the Soret number Sr , the heat source sink β and the Eckert number Ec increase.

6. Applications

This problem may be useful in the following fields

- i. Juice production
- ii. Pizza sauce dispensing
- iii. Vitamin A & D injection
- iv. Ultra-filtration
- v. Transfer of fuels and lubricants

Acknowledgement

No funding for this project. These authors would like to thank the reviewer for their valuable remarks.

References

- [1] Srinivasacharya, D., G. Radhakrishnamacharya, and C. H. Srinivasulu. "The effects of wall properties on peristaltic transport of a dusty fluid." *Turkish Journal of Engineering and Environmental Sciences* 32, no. 6 (2009): 357-365.
- [2] Reddy, M. Suryanarayan, G. Sankar Shekar Raju, MV Subba Reddy, and K. Jayalakshmi. "Peristaltic MHD flow of a Bingham fluid through a porous medium in a channel." *African Journal of Scientific Research* 3, no. 1 (2011): 179-203.
- [3] Abou-zeid, Mohamed Y., and Mona AA Mohamed. "Homotopy perturbation method for creeping flow of non-Newtonian power-law nanofluid in a nonuniform inclined channel with peristalsis." *Zeitschrift für Naturforschung A* 72, no. 10 (2017): 899-907.
<https://doi.org/10.1515/zna-2017-0154>
- [4] Mekheimer, Kh S. "The influence of heat transfer and magnetic field on peristaltic transport of a Newtonian fluid in a vertical annulus: application of an endoscope." *Physics letters A* 372, no. 10 (2008): 1657-1665.
<https://doi.org/10.1016/j.physleta.2007.10.028>
- [5] El-dabe, Nabil Tawfik, Mohamed Yahya Abou-zeid, and Ola S. Ahmed. "Motion of a Thin Film of a Fourth Grade Nanofluid with Heat Transfer Down a Vertical Cylinder: Homotopy Perturbation Method Application." *Journal of Advanced Research in Fluid Mechanics and Thermal Sciences* 66, no. 2 (2020): 101-113.
- [6] Eldabe, Nabil TM, Mohamed A. Hassan, and Mohamed Y. Abou-Zeid. "Wall properties effect on the peristaltic motion of a coupled stress fluid with heat and mass transfer through a porous medium." *Journal of engineering mechanics* 142, no. 3 (2016): 04015102.

- [https://doi.org/10.1061/\(ASCE\)EM.1943-7889.0001029](https://doi.org/10.1061/(ASCE)EM.1943-7889.0001029)
- [7] Medhavi, Amit. "Peristaltic pumping of a non-Newtonian fluid." *Applic. and Appl. Math* 3 (2008): 137-148.
- [8] Rani, P. Naga, and G. Sarojamma. "Peristaltic transport of a Casson fluid in an asymmetric channel." *Australasian Physics & Engineering Sciences in Medicine* 27, no. 2 (2004): 49.
<https://doi.org/10.1007/BF03178376>
- [9] Mansour, Hesham Mohamed, and Mohamed Y. Abou-zeid. "Heat and Mass Transfer Effect on Non-Newtonian Fluid Flow in a Non-uniform Vertical Tube with Peristalsis." *Journal of Advanced Research in Fluid Mechanics and Thermal Sciences* 61, no. 1 (2019): 44-62.
- [10] Attia, Hazem Ali. "Unsteady Hartmann flow with heat transfer of a viscoelastic fluid considering the Hall effect." *Canadian Journal of Physics* 82, no. 2 (2004): 127-139.
<https://doi.org/10.1139/p03-117>
- [11] Asghar, S., Muhammad R. Mohyuddin, and T. Hayat. "Effects of Hall current and heat transfer on flow due to a pull of eccentric rotating disks." *International Journal of Heat and Mass Transfer* 48, no. 3-4 (2005): 599-607.
<https://doi.org/10.1016/j.ijheatmasstransfer.2004.08.023>
- [12] Hayat, T., N. Ali, and S. Asghar. "Hall effects on peristaltic flow of a Maxwell fluid in a porous medium." *Physics Letters A* 363, no. 5-6 (2007): 397-403.
<https://doi.org/10.1016/j.physleta.2006.10.104>
- [13] Abo-Eldahab, E. M., E. I. Barakat, and K. I. Nowar. "Hall currents and ion-slip effects on the MHD peristaltic transport." *International Journal of Applied Mathematics and Physics* 2, no. 2 (2010): 113-123.
- [14] Abo-Eldahab, E. M., E. I. Barakat, and K. I. Nowar. "Effects of Hall and ion-slip currents on peristaltic transport of a couple stress fluid." *International Journal of Applied Mathematics and Physics* 2, no. 2 (2010): 145-157.
- [15] Eldabe, Nabil Tawfik, Galal M. Moatimid, Mohamed Abouzeid, Abdelhafeez A. El-Shehpiy, and Naglaa Fawzy Abdallah. "Instantaneous Thermal-Diffusion and Diffusion-Thermo Effects on Carreau Nanofluid Flow Over a Stretching Porous Sheet." *Journal of Advanced Research in Fluid Mechanics and Thermal Sciences* 72, no. 2 (2020): 142-157.
<https://doi.org/10.37934/arfmts.72.2.142157>
- [16] Dursunkaya, Zafer, and William M. Worek. "Diffusion-thermo and thermal-diffusion effects in transient and steady natural convection from a vertical surface." *International Journal of heat and mass transfer* 35, no. 8 (1992): 2060-2065.
[https://doi.org/10.1016/0017-9310\(92\)90208-A](https://doi.org/10.1016/0017-9310(92)90208-A)
- [17] Postelnicu, Adrian. "Influence of a magnetic field on heat and mass transfer by natural convection from vertical surfaces in porous media considering Soret and Dufour effects." *International Journal of Heat and Mass Transfer* 47, no. 6-7 (2004): 1467-1472.
<https://doi.org/10.1016/j.ijheatmasstransfer.2003.09.017>
- [18] Alam, M. S., M. M. Rahman, and M. A. Samad. "Numerical study of the combined free-forced convection and mass transfer flow past a vertical porous plate in a porous medium with heat generation and thermal diffusion." *Nonlinear Analysis* 11, no. 4 (2006): 331-343.
<https://doi.org/10.15388/NA.2006.11.4.14737>
- [19] Eldabe, Nabil, and Mohamed Abou-Zeid. "Radially varying magnetic field effect on peristaltic motion with heat and mass transfer of a non-Newtonian fluid between two co-axial tubes." *Thermal Science* 22, no. 6 Part A (2018): 2449-2458.
<https://doi.org/10.2298/TSCI160409292E>
- [20] Abou-Zeid, Mohamed Y. "Homotopy perturbation method for couple stresses effect on MHD peristaltic flow of a non-Newtonian nanofluid." *Microsystem Technologies* 24, no. 12 (2018): 4839-4846.
<https://doi.org/10.1007/s00542-018-3895-1>
- [21] Eldabe, Nabil T., Raafat R. Rizkalla, Mohamed Y. Abouzeid, and Vivian M. Ayad. "Thermal diffusion and diffusion thermo effects of Eyring-Powell nanofluid flow with gyrotactic microorganisms through the boundary layer." *Heat Transfer—Asian Research* 49, no. 1 (2020): 383-405.
<https://doi.org/10.1002/htj.21617>
- [22] Abou-Zeid, M. Y. "Homotopy perturbation method to gliding motion of bacteria on a layer of power-law nanoslime with heat transfer." *Journal of Computational and Theoretical Nanoscience* 12, no. 10 (2015): 3605-3614.
<https://doi.org/10.1166/jctn.2015.4246>
- [23] Abou-Zeid, Mohamed Y., Abeer A. Shaaban, and Muneer Y. Alnour. "Numerical treatment and global error estimation of natural convective effects on gliding motion of bacteria on a power-law nanoslime through a non-Darcy porous medium." *Journal of Porous Media* 18, no. 11 (2015).
<https://doi.org/10.1615/JPorMedia.2015012459>

-
- [24] Abou-zeid, Mohamed Y. "Magnetohydrodynamic boundary layer heat transfer to a stretching sheet including viscous dissipation and internal heat generation in a porous medium." *Journal of porous Media* 14, no. 11 (2011).
<https://doi.org/10.1615/JPorMedia.v14.i11.50>
- [25] Mohamed, Mona AA, and Mohamed Y. Abou-zeid. "MHD peristaltic flow of micropolar Casson nanofluid through a porous medium between two co-axial tubes." *Journal of Porous Media* 22, no. 9 (2019).
<https://doi.org/10.1615/JPorMedia.2018025180>
- [26] M. J. Lighthill. "Introduction to Fourier analysis and generalised functions." *Bulletin of the American Mathematical Society* 65, no. 4 (1959): 248-249.
<https://doi.org/10.1090/S0002-9904-1959-10325-6>
- [27] Wahid, Nur Syahirah, Mohd Ezad Hafidz Hafidzuddin, Norihan Md Arifin, Mustafa Turkyilmazoglu, and Nor Aliza Abd Rahmin. "Magnetohydrodynamic (MHD) Slip Darcy Flow of Viscoelastic Fluid Over A Stretching Sheet and Heat Transfer with Thermal Radiation and Viscous Dissipation." *CFD Letters* 12, no. 1 (2020): 1-12.